

Nonequilibrium Corrections to the Spectra of Massless Neutrinos in the Early Universe.

A.D. Dolgov^{1 2}, S.H. Hansen³

Teoretisk Astrofysik Center

Juliane Maries Vej 30, DK-2100, Copenhagen, Denmark

D.V. Semikoz⁴

Institute of Nuclear Research of the Russian Academy of Sciences

60th October Anniversary Prospect 7a , Moscow 117312, Russia

Abstract

Distortion of the equilibrium spectra of cosmic neutrinos due to interaction with hotter electrons and positrons in the primeval cosmic plasma is considered. The set of integro-differential kinetic equations for neutrinos is accurately numerically solved. The relative corrections to neutrino energy densities are approximately 0.9% for ν_e and 0.4% for ν_μ and ν_τ . This effect results in $1.4 \cdot 10^{-4}$ increase in the primordial ${}^4\text{He}$ abundance.

¹Also: ITEP, Bol. Cheremushkinskaya 25, Moscow 113259, Russia.

²e-mail: dolgov@tac.dk

³e-mail: sthansen@tac.dk

⁴e-mail: semikoz@ms2.inr.ac.ru

1 Introduction

At high temperatures the primeval cosmic plasma is very close to equilibrium. This is because the reaction rate, $\Gamma = \sigma n$, typically is much higher than the expansion rate, $H \sim 1/t$. Here σ is the characteristic cross-section and $n \sim T^3$ is the particle number density. One can see from the covariant Boltzmann kinetic equation:

$$(\partial_t - Hp\partial_p)f = I_{coll} \quad (1)$$

that equilibrium for massless particles is not distorted by the expansion of the universe. Indeed the equilibrium distribution:

$$f_{eq} = [\exp(E - \mu(t))/T(t) \pm 1]^{-1} \quad (2)$$

which annihilates the collision integral I_{coll} , satisfies this equation if $\dot{T}/T = -H$ and $\mu(t) \sim T(t)$. However if the particle mass m is nonzero, the l.h.s. of eq. (1) cannot vanish for all possible values of the momentum p with any choice of the functions $T(t)$ and $\mu(t)$. The deviation from equilibrium can roughly be estimated as $\delta f/f = Hm^2/(\Gamma TE)$.

Since photons and electrons are very strongly coupled, the deviations from equilibrium in the electromagnetic cosmic plasma are tiny. This is the reason for a perfect Planckian shape in the observed spectrum of the cosmic microwave radiation, where the distortion is known to be smaller than 10^{-4} . One would expect the same to be true for massless cosmic neutrinos. However this is not so and the spectral corrections, especially in the high energy tail, can be of several per cent. The physics of the phenomenon is quite simple. At high temperatures neutrinos and electrons are sufficiently strongly coupled to each other, they have the equilibrium distributions and their temperatures are equal. At smaller temperatures, below 2-3 MeV, the neutrinos decouple and below these temperatures the primeval plasma consists of two (or better to say four) almost decoupled components, the electromagnetic and three neutrino ones. In the approximation of instantaneous decoupling the neutrino spectra maintain their equilibrium shape with the temperature decreasing as the inverse

scale factor, $T_\nu \sim 1/a(t)$. The temperature of electrons and photons decreases slower because e^+e^- -annihilation heats up the electromagnetic part of the plasma when the temperature drops below m_e . Ultimately the ratio of the temperatures reaches the well known value $T_\gamma/T_\nu = (11/4)^{1/3} = 1.401$, see e.g. ref. [1]. This result was obtained under the assumption of entropy conservation in the electromagnetic sector, which is not necessarily true in the non-equilibrium case, where the limiting value of T_γ/T_ν becomes slightly different. The interactions between the electromagnetic and neutrino components of the plasma, though weak, are not completely vanishing and therefore the residual annihilation $e^+e^- \rightarrow \nu\bar{\nu}$ and, to a lesser extend, elastic scattering $e\nu \rightarrow e\nu$ slightly heat up the neutrinos and distort their spectra. The distortions are larger at higher energies because the weak interactions are getting stronger with rising energy.

The overall neutrino heating under assumption of equilibrium spectra has been considered earlier in refs. [2, 3, 4]. In this approximation the problem is very much simplified but the method itself is far from being precise from the very beginning. A more complete approach with the distortion of the spectra taken into account has been discussed in several papers [5, 6, 7] in different approximations and with somewhat different results. In what follows we present an accurate numerical treatment of the problem with a better accuracy than that of the preceding paper [7] where the numerical solutions of the exact kinetic equations were also obtained. Our better accuracy is achieved by a convenient reduction of the collision integral to two dimensions and a powerful integration method developed in ref. [8].

2 Basic Equations

Instead of time and momenta we choose the following dimensionless variables:

$$x = ma(t), \quad y_j = p_j a(t) \tag{3}$$

where m is an arbitrary parameter with dimension of mass, which we took as $m = 1$ MeV and the scale factor $a(t)$ is normalized so that $a(t) = 1/T_\nu = 1/T_\gamma$ at high temperatures or at early times. In terms of these variables the kinetic equation (1) can be rewritten as:

$$Hx\partial_x f(x, y_1) = I_{coll}. \quad (4)$$

The collision integral I_{coll} is dominated by two-body reactions $1 + 2 \rightarrow 3 + 4$ and is given by the expression:

$$I_{coll} = \frac{1}{2E_1} \sum \int \frac{d^3p_2}{2E_2(2\pi)^3} \frac{d^3p_3}{2E_3(2\pi)^3} \frac{d^3p_4}{2E_4(2\pi)^3} (2\pi)^4 \delta^{(4)}(p_1 + p_2 - p_3 - p_4) F(f_1, f_2, f_3, f_4) S |A|_{12 \rightarrow 34}^2 \quad (5)$$

where $F = f_3 f_4 (1 - f_1)(1 - f_2) - f_1 f_2 (1 - f_3)(1 - f_4)$, $|A|^2$ is the weak interaction amplitude squared summed over spins of all particles except the first one, and S is the symmetrization factor which includes $1/2!$ for each pair of identical particles in initial and final states and the factor 2 if there are 2 identical particles in the initial state; the summation is done over all possible sets of leptons 2, 3, and 4; The relevant reactions are presented in Table 1 for the case when the first particle is ν_e , and in Table 2 for ν_μ or ν_τ . Our results in these tables agree with those of ref. [7] except for the reactions $\nu_a \nu_a \rightarrow \nu_a \nu_a$ where we took twice larger contribution because of identical particles in the initial state.

We assume that the distribution functions for ν_μ and ν_τ are equal while that for ν_e is different because of different strength of charged current interactions. Similarly we assume that the lepton asymmetry is negligible so that $f_\nu = f_{\bar{\nu}}$. Therefore there are two unknown functions of x and y : f_{ν_e} and $f_{\nu_\mu} = f_{\nu_\tau}$. Each of them satisfies the kinetic equation (4) with the appropriate collision integral. We also assume that the distributions of photons and electrons are the exact equilibrium ones (2) with the unknown temperature $T_\gamma(x)$ and zero chemical potential, $\mu(x) = 0$. The third necessary equation is the covariant energy conservation:

$$x \frac{d\rho(x)}{dx} = -3(\rho + P) \quad (6)$$

where ρ is the total energy density:

$$\rho = \frac{\pi^2 T_\gamma^4}{15} + \frac{2}{\pi^2} \int \frac{dq q^2 \sqrt{q^2 + m_e^2}}{\exp(E/T_\gamma) + 1} + \frac{1}{\pi^2} \int dq q^3 f_{\nu_e} + \frac{2}{\pi^2} \int dq q^3 f_{\nu_\mu} \quad (7)$$

and P is the pressure:

$$P = \frac{\pi^2 T_\gamma^4}{45} + \frac{2}{\pi^2} \int \frac{dq q^4}{3\sqrt{q^2 + m_e^2}[\exp(E/T_\gamma) + 1]} + \frac{1}{3\pi^2} \int dq q^3 f_{\nu_e} + \frac{2}{3\pi^2} \int dq q^3 f_{\nu_\mu} \quad (8)$$

The Hubble parameter, $H = \dot{a}/a$, which enters the kinetic equation (4) is expressed through ρ in the usual way, $3H^2 m_{Pl}^2 = 8\pi\rho$, ignoring the curvature term and the cosmological constant.

The collision integral in eq. (5) can be reduced from nine to two dimensions as described in Appendix A. For the sake of brevity let us introduce some notations: $f_a(p_j) \equiv f_a^{(j)}$, $d_1 = D_1$, $d_2(3,4) = D_2(3,4)/E_3 E_4$, and $d_3 = D_3/E_1 E_2 E_3 E_4$. The functions D_j are defined in Appendix A. We do not indicate the arguments for the functions D_1 and D_3 because they are symmetric in all 4 arguments. In terms of these functions we can write the coupled kinetic equations for f_{ν_e} and f_{ν_μ} in the following way:

$$\begin{aligned} Hx\partial_x f_{\nu_e}^{(1)} &= \frac{G_F^2}{2\pi^3 p_1} \int dp_2 p_2 dp_3 p_3 dp_4 p_4 \delta(E_1 + E_2 - E_3 - E_4) \\ &\left\{ F[f_{\nu_e}^{(1)}, f_{\nu_e}^{(2)}, f_{\nu_e}^{(3)}, f_{\nu_e}^{(4)}] [6d_1 - 4d_2(1,4) - 4d_2(2,3) + 2d_2(1,2) + 2d_2(3,4) + 6d_3] \right. \\ &+ F[f_{\nu_e}^{(1)}, f_{\nu_\mu}^{(2)}, f_{\nu_e}^{(3)}, f_{\nu_\mu}^{(4)}] [4d_1 + 2d_2(1,2) + 2d_2(3,4) - 2d_2(1,4) - 2d_2(2,3) + 4d_3] \\ &+ F[f_{\nu_e}^{(1)}, f_{\nu_e}^{(2)}, f_{\nu_\mu}^{(3)}, f_{\nu_\mu}^{(4)}] [2d_1 - 2d_2(2,3) - 2d_2(1,4) + 2d_3] \\ &+ F[f_{\nu_e}^{(1)}, f_e^{(2)}, f_{\nu_e}^{(3)}, f_e^{(4)}] [4(g_L^2 + g_R^2)(2d_1 - d_2(2,3) - d_2(1,4) + d_2(3,4) \\ &\quad + d_2(1,2) + 2d_3) - 8g_L g_R m_e^2 (d_1 - d_2(1,3))/E_2 E_4] \\ &\left. + F[f_{\nu_e}^{(1)}, f_{\nu_e}^{(2)}, f_e^{(3)}, f_e^{(4)}] [4g_L^2 (d_1 - d_2(2,3) - d_2(1,4) + d_3) + \right. \\ &\left. 4g_R^2 (d_1 - d_2(2,4) - d_2(1,3) + d_3) + 4g_L g_R m_e^2 (d_1 + d_2(1,2))/E_3 E_4] \right\} \quad (9) \end{aligned}$$

and:

$$Hx\partial_x f_{\nu_\mu}^{(1)} = \frac{G_F^2}{2\pi^3 p_1} \int dp_2 p_2 dp_3 p_3 dp_4 p_4 \delta(E_1 + E_2 - E_3 - E_4)$$

$$\begin{aligned}
& \left\{ F[f_{\nu_\mu}^{(1)}, f_{\nu_\mu}^{(2)}, f_{\nu_\mu}^{(3)}, f_{\nu_\mu}^{(4)}][9d_1 - 6d_2(1, 4) - 6d_2(2, 3) + 3d_2(1, 2) + 3d_2(3, 4) + 9d_3] \right. \\
& \quad + F[f_{\nu_\mu}^{(1)}, f_{\nu_e}^{(2)}, f_{\nu_\mu}^{(3)}, f_{\nu_e}^{(4)}][2d_1 + d_2(1, 2) + d_2(3, 4) - d_2(1, 4) - d_2(2, 3) + 2d_3] \\
& \quad \quad + F[f_{\nu_\mu}^{(1)}, f_{\nu_\mu}^{(2)}, f_{\nu_e}^{(3)}, f_{\nu_e}^{(4)}][d_1 - d_2(2, 3) - d_2(1, 4) + d_3] \\
& \quad \quad + F[f_{\nu_\mu}^{(1)}, f_e^{(2)}, f_{\nu_\mu}^{(3)}, f_e^{(4)}][4(\tilde{g}_L^2 + g_R^2)(2d_1 - d_2(2, 3) - d_2(1, 4) + d_2(3, 4) \\
& \quad \quad \quad + d_2(1, 2) + 2d_3) - 8\tilde{g}_L g_R m_e^2(d_1 - d_2(1, 3))/E_3 E_4] \\
& \quad \quad + F[f_{\nu_\mu}^{(1)}, f_{\nu_\mu}^{(2)}, f_e^{(3)}, f_e^{(4)}][4\tilde{g}_L^2(d_1 - d_2(2, 3) - d_2(1, 4) + d_3) + \\
& \quad \quad \quad \left. 4g_R^2(d_1 - d_2(2, 4) - d_2(1, 3) + d_3) + 4\tilde{g}_L g_R m_e^2(d_1 + d_2(1, 2))/E_3 E_4] \right\}, \quad (10)
\end{aligned}$$

where $g_L = 1/2 + \sin^2 \theta_W$, $g_R = \sin^2 \theta_W$ and $\tilde{g}_L = -1/2 + \sin^2 \theta_W$, $f_e = [\exp(E/T_\gamma) + 1]^{-1}$, and the temperature T_γ is determined from eq. (6). Thus we have the complete system of three equations for three unknown functions $T_\gamma(x)$, $f_{\nu_e}(x, y)$, and $f_{\nu_\mu}(x, y)$ which we solve numerically. The solution has been found in two different but equivalent ways. First, the system has been solved directly, as it is, for the full distribution functions $f_{\nu_j}(x, y)$ and, second, for the small deviations δ_j from equilibrium $f_{\nu_j}(x, y) = f_{\nu_j}^{(eq)}(y)(1 + \delta_j(x, y))$, where $f_{\nu_j}^{(eq)} = [\exp(E/T_\nu) + 1]^{-1}$ with $T_\nu = 1/a$. In both cases the numerical solution has been done exactly, not perturbatively. So with infinitely good numerical precision the results must be the same. However since the precision is finite, different ways may give different results and their consistency is a good check of the accuracy of the calculations. It is convenient to introduce $\delta(x, y)$ because the dominant terms in the collision integrals, containing neutrinos only, cancel and subdominant terms are proportional to δ . In the parts of the collision integrals which contain electrons, there are also contributions proportional to the difference in temperatures ($T_\gamma - T_\nu$). We have found that the results of these two methods, i.e. solving either for f_ν or δ , are very close (see the next Section and Table 3).

To check possible algebraic errors we have made the following procedure. First, we have solved numerically the three relevant equations in the Boltzmann approximation, simply changing the function F which is defined after eq. (5) to $F \rightarrow f_3 f_4 - f_1 f_2$ with the same coefficients and d-functions in the collision integral as presented above.

Second, we repeated the numerical calculation but this time we changed the terms describing the direct reactions (the ones that enter I_{coll} with negative signs) with (presumably) identical terms where the integration over the phase space of the final particles had been made explicitly. That is, the positive terms were described through d-functions as above, while negative ones had been calculated in a different and independent way. The expressions for the negative terms are presented in Appendix B. The results of these two numerical calculations are in perfect agreement. This excludes possible accidental errors in calculations of D-functions (see Appendix A) as well as in the typing of the program for the numerical integration.

3 Description of Calculations and Results

3.1 Initial conditions

We have numerically calculated the evolution of the distribution functions satisfying the system of eqs. (6,9,10) in terms of the dimensionless time $x = m_0 a$ in the interval $x_{in} \leq x \leq x_f$, where a is the scale factor. With our normalization the "time" $x = 1$ corresponds to the neutrino temperature $T_\nu = m_0 = 1MeV$.⁵

For large values of x the collision integrals in the r.h.s. of eqs. (9,10) are suppressed by the factor $1/x^2$. We have found that at $x \approx 50$ all the functions f_{ν_e} , $f_{\nu_{\mu(\tau)}}$, and T_γ reach their asymptotic values, so to be certain that we are in the asymptotic limit we have chosen the final time $x_f = 60$. For the initial time x_{in} we have chosen three different values $x_{in} = 0.1, 0.2,$ and 0.5 which correspond to $T_\nu = 10MeV, 5MeV,$ and $2MeV$ respectively. In all the cases we have assumed that the neutrinos are in thermal equilibrium for $x \leq x_{in}$ with the distribution functions $f_{\nu_j}^{(eq)} = 1/[\exp(y) + 1]$.

For the dimensionless momentum $y = pa$ we took a 100 and a 200 point grid, equally spaced in the region $0 \leq y \leq 20$. In contrast to ref. [7] we have included the

⁵Strictly speaking for non-equilibrium neutrinos we cannot introduce temperature T_ν . But since non-equilibrium corrections to the neutrino spectrum are small (see below) we sometimes use the notation T_ν instead of $1/a$, because in equilibrium $T_\nu a = 1$.

point $y = 0$ in which the collision integrals in eqs. (9,10) have different analytical expressions due to the cancellation of the factor $1/p_1^2$ in front of the collision integrals by the corresponding factors in the functions D_i . This allows us to compare the collision integral at $y = 0$ with the integral in a nearby point $0 < y \ll 1$ in order to check that the numerical errors are small in the region of small momenta $y < 1$.

3.2 Numerical results

There are three phenomena which play essential roles in the evolution of the neutrino distribution functions. The first of them is the temperature difference between photons and e^\pm on one side and neutrinos on the other, which arises due to the heating of the electromagnetic plasma by e^+e^- -annihilation. Through the interactions of neutrinos with electrons this temperature difference leads to non-equilibrium distortions of the neutrino spectra. The temperature difference is essential in the interval $1 < x < 30$. The second effect is the freezing of the neutrino interactions because the collision integrals in the r.h.s. of eqs. (9,10) drop as $1/x^2$. At small $x \ll 1$ the collisions are very efficient but at $x > 1$ they are strongly suppressed. The third important phenomenon is the elastic $\nu\nu$ -scattering which smoothes down the non-equilibrium corrections to the neutrino spectrum. It is especially important at small $x < 1$.

Accordingly, the evolution of the distribution functions proceeds as follows. At $x < 0.2$ the temperature difference is negligibly small while $\nu\nu$ -scattering is strong. Therefore the neutrino distribution functions are practically in equilibrium. In the interval $0.2 \leq x \leq 4$ all three effects are essential and during this period the neutrino spectra are distorted and simultaneously the photon temperature slightly drops down because of the energy transfer from e^\pm to neutrinos, as compared to the photon temperature in the approximation where the neutrino decoupling is instantaneous. When $x > 4$ the collision integrals in the r.h.s. of eqs. (9,10) are small and the temperature difference practically does not affect the neutrino distribution functions,

even though the temperature difference is the largest in this time interval.

In Figs. 1-5 we present the results of the numerical solution of the system of eqs. (6,9,10) in the interval $0.1 \leq x \leq 60$ (approximately 4000 points in x) both for Fermi-Dirac (FD) and Maxwell-Boltzmann (MB) statistics. In these runs we used a 100 point grid in the momentum interval $0 \leq y \leq 20$.

The ratio T_γ/T_ν as a function of x is presented in Fig. 1 for FD and MB statistics. If we neglect the exchange of energy between e^\pm and neutrinos in eq. (6) (which is equivalent to entropy conservation) the asymptotic values are $T_\gamma/T_\nu = 1.4010$ for FD statistics and $T_\gamma/T_\nu = 1.4423$ for MB statistics. When the energy exchange is taken into account (energy conservation) these ratios have slightly different values $T_\gamma/T_\nu = 1.3991$ (or 1.3994, using the full distribution function) for FD statistics and $T_\gamma/T_\nu = 1.4404$ for MB statistics.

In Fig. 2 the correction to the total neutrino energy density $\delta\rho_\nu/\rho_{eq}$ for the case of FD statistics is plotted. Here $\rho_{eq} = (7\pi^2/240)(m/x)^4$ is the unperturbed energy density of neutrinos and:

$$\delta\rho_\nu = \frac{\rho_{\nu_e} + 2\rho_{\nu_\mu}}{3} - \rho_{eq} , \quad (11)$$

with ρ_{ν_e} and ρ_{ν_μ} found from our numerical solution. The upper curve in Fig. 2 corresponds to the entropy conservation case, while the lower one corresponds to the energy conservation case. The effect is smaller in the second case because the "driving force", which is proportional to the temperature difference, is lower due to the excessive photon cooling. We can see that while the difference in the asymptotic values of T_γ/T_ν for these two cases is as small as 0.14% the difference in $\delta\rho_\nu/\rho_{eq}$ is as large as 20%. This can be explained in the following way. Compare Fig. 1 and Fig. 2 for the FD case. We see that already at $x = 4$ the value of the function $\delta\rho_\nu/\rho_{eq}$ is close to its asymptotic value. At the same moment, $x = 4$, the ratio T_γ/T_ν has a value of 1.08 which is much smaller than the asymptotic one, 1.401. This means that the dominant contribution to the distortion of the neutrino spectra comes from the period when the temperature difference $\Delta T = T_\gamma - T_\nu$ was rather small. The

smallness of ΔT was compensated by a more efficient energy exchange between ν and e^\pm at smaller x . In this range of x , a relatively small variations in T_γ/T_ν connected to different approximations made in the calculations, should be compared with the small difference ΔT . Thus a small variation in T_γ/T_ν is relatively enhanced, and we see how these small variations can produce the strong 20% effect.

In Fig. 3 the relative deviations of the neutrino spectra from the equilibrium one, $\delta_j(x, y) = (f_{\nu_j} - f_{eq})/f_{eq}$, are presented as functions of x for several values of the momentum $y = 3, 5, 7$. In Fig. 3a we present the results for electronic neutrinos and in Fig. 3b for muonic (tau) ones. For large momenta y the deviation from the equilibrium is larger and the maximum asymptotic value is reached later (at larger x). This is a result of stronger interactions of more energetic neutrinos.

In Fig. 4 we compare the deviations from the equilibrium distributions, δ_{ν_e} and $\delta_{\nu_{\mu(\tau)}}$ for FD and MB statistics. We plot δ_i for the same value of the momentum $y = 5$ as functions of x . We see that the results for the case of Boltzmann statistics are larger than those for the Fermi one by approximately 25%. For both FD and MB statistics the spectral distortion for ν_e is more than twice larger than that for ν_μ or ν_τ . This is due to a stronger coupling of ν_e to e^\pm .

In Fig. 5 we plot the asymptotic values of the corrections to the neutrino distributions $\delta_j = (f_{\nu_j} - f_{\nu_j}^{eq})/f_{\nu_j}^{eq}$ as functions of the dimensionless momentum y . The dashed lines a and c correspond to Maxwell-Boltzmann statistics and the solid lines b and d correspond to Fermi-Dirac statistics. The upper curves a and b are for electronic neutrinos and the lower curves c and d are for muonic (tau) neutrinos. All the curves can be well approximated by a second order polynomial in y like $\delta = Ay(y - B)$ in agreement with ref. [5].

3.3 Checking the results

First, let us discuss the choice of the initial time x_{in} . We made the runs for the system of eqs. (6,9,10) with three different values $x_{in} = 0.1, 0.2$ and 0.5 . We found that the

results of the runs with $x_{in} = 0.1$ and $x_{in} = 0.2$ are the same with the accuracy of 10^{-5} in the distribution function for all values of x (see Table 3). This means that for $x \leq 0.2$ we can neglect the non-equilibrium corrections to the neutrino distribution functions. For larger x this is not so and e.g. the spectral distortion calculated with $x_{in} = 0.5$ is smaller by approximately 15% than the one calculated with $x_{in} = 0.2$.

In order to check the errors connected with a finite number of points in the momentum interval $0 \leq y \leq 20$ we took a 100 and a 200 point grids. We found that the difference in the results is small, which means that a 100 points grid is a good approximation for the numerical solution of our system of kinetic equations.

The errors connected with a finite number of points in time x are much more important. We control these errors in the following way. First, we run the program with some fixed number of points in time x , distributed in the time interval $x_{in} < x < x_f$ in such a way that the distribution functions do not change significantly at any momentum point y during one time iteration dx . Then we run the program for the entropy conservation law (i.e. with equilibrium neutrinos) with the same values of time x_i as in the first run. Then we compare the asymptotic values of the temperature ratios with the sample values which are $T_\gamma/T_\nu = (11/4)^{1/3} = 1.4010$ for FD statistics and $T_\gamma/T_\nu = 3^{1/3} = 1.44225$ for MB statistics. We found that when we run with 400 time points, the numerical error in these temperature ratios are of the order ~ 0.001 , and this value is only one order of magnitude smaller than the effect itself, which is not good enough. However, in the case of 4000 time points this error is as small as $\sim 10^{-4}$. In our calculations we used a 4000 point grid in time.

We also checked the errors related to the finite number of points in time in a different way. Instead of the simple time evolution we used the Bulirsch-Stoer method, described in the book [9]. We found, that this method gives the same results as the simple time evolution with 4000 time points (see the first two rows in Table 3).

Besides reducing the numerical errors we have used two different analytical approaches in order to check the results. In the case of FD statistics we solve the system

of eqs. (6,9,10) both for the full neutrino distribution functions f_{ν_j} and for the deviations from equilibrium $\delta_j = (f_{\nu_j} - f_{\nu}^{eq})/f_{\nu}^{eq}$. In the last case the contributions to the collision integrals for all the processes vanish for vanishing δ , except for the interactions of neutrinos with electrons, where the "driving force" term, proportional to the temperature difference between ν and e^{\pm} , gives a nonzero contribution. Comparing the results in these two cases (with the same values of all parameters) we have found that the non-equilibrium corrections to the neutrino spectra are systematically smaller by about 10% when the equations are solved for the full distribution functions f_{ν_j} . The comparison of the results of the different ways of calculation are summarized in Table 3.

3.4 Helium abundance

We have modified the standard nucleosynthesis code (ref. [10]) in the following way. The neutrino distribution functions have been parametrized as:

$$f_{\nu_i} \rightarrow f_{\nu_i} \cdot (1 + \delta_i(p, T_{\nu})), \quad (12)$$

where δ_i were fitted as functions of momentum and temperature in accordance with our numerical solutions.

First, the neutrino energy densities ρ_{ν_i} have been calculated with the corrected spectra. This changes the universe cooling rate and has the major impact on the helium abundance.

Second, the 6 weak interaction rates for ($n \leftrightarrow p$)-reactions have been modified with the account for the spectral distortion of the electronic neutrinos. The 3 reactions with ν_e or $\bar{\nu}_e$ in the initial state, $n \nu_e \rightarrow p e^-$, $p \bar{\nu}_e \rightarrow n e^+$ and $p \bar{\nu}_e e^- \rightarrow n$, are more important and the neutrino distribution functions have been corrected according to eq. (12). However, for the 3 inverse reactions with neutrinos in the final state, $n e^+ \rightarrow p \bar{\nu}$, $n \rightarrow p e^- \bar{\nu}$ and $p e^- \rightarrow n \nu$, the spectral modification results only in a small correction to the Pauli suppression factor, $(1 - f_{\nu}) \rightarrow (1 - f_{\nu} \cdot (1 + \delta))$, and the effect of the corrections to these last 3 reactions is negligible.

Finally the law of the evolution of the photon temperature is slightly changed, which in turn also affects the reaction rates. The correct photon temperature is calculated by including the neutrino energy densities into the equation governing the variation of the photon temperature in the course of the universe expansion:

$$\frac{dT_\gamma}{d \ln V} = -\frac{\rho_{EM} + p_{EM} + 4/3 \rho_\nu}{d\rho_{EM}/dT_\gamma + d\rho_\nu/dT_\gamma}, \quad (13)$$

where $V = a^3$. If neutrinos had the equilibrium distribution their energy density would satisfy the covariant conservation law (6) separately so that their contribution into eq. (13) would cancel out. However this is not true if the energy exchange between ν 's and e^\pm is taken into account.

The final change in helium-4 abundance has been found to be $\Delta Y = 1.4 \cdot 10^{-4}$. Similarly we find relative changes in the ${}^3\text{He}$ and ${}^7\text{Li}$ abundances of the order $5 \cdot 10^{-4}$ and $-6 \cdot 10^{-4}$ respectively.

4 Discussion

Our results agree reasonably well with the previous numerical calculations of ref. [7]. For example we obtain $\delta\rho_{\nu_e}/\rho_{\nu_e} = 0.94\%$ (0.83%) and $\delta\rho_{\nu_\mu}/\rho_{\nu_\mu} = 0.40\%$ (0.33%) (see Table 3), to be compared with 0.83% and 0.41% respectively obtained in ref. [7]. For the shape of the spectral distortion the difference is larger, especially for low y . To characterize the difference let us introduce the effective neutrino temperature as $T_{eff} = E/\ln[(1-f)/f]$, which we compare to the unperturbed temperature T_0 calculated in the limit of entropy conservation i.e. in neglect of the neutrino heating. The difference:

$$\frac{T_{eff} - T_0}{T_0} = \frac{1 - e^{-y}}{y} \delta(x, y) \quad (14)$$

goes to a small negative value for small y in our case and to a considerably larger positive one according to ref. [7]. We ascribe this difference to a better accuracy of our calculations which is most profound at low y (in particular we took a 100-200 point grid in comparison to 35 in ref. [7]). The physical reason for this negative result

is the elastic νe^\pm -scattering. Since electrons and positrons have a slightly higher temperature than the neutrinos, the scattering will depopulate the low momentum region pushing neutrinos to higher momenta. Our agreement with ref. [7] is much better for the physically more important region of high y . The distribution function decreases exponentially, whereas the correction δ increases quadratically. Moreover the weak interaction rates are typically proportional to the energy squared, so the dominant contribution of δ to neutron-proton reactions lays near $y = 5$. For large y our results are systematically larger than that of ref. [7] by approximately 15%. This difference cannot be ascribed to the difference by a factor two in the collision integrals for the scattering of identical neutrinos because that leads to the opposite sign of the effect and is rather small, giving corrections of a few per cent. We believe that the difference between us and ref. [7] arises because of different numerical accuracies.

Another source of the difference in the results is the different treatment of the cooling of the electromagnetic plasma. The simplest approach is to neglect the loss of photon energy which goes into neutrinos. In this case the entropy of photons and e^+e^- -pairs is conserved and the function $T_\gamma(x)$ can be determined from the relation $x^3(\rho_{em} + P_{em})/T_\gamma = const$. In this approximation the cooling of the electromagnetic plasma is induced only by the expansion of the universe. The energy transmitted to neutrinos results in an excessive cooling which we have calculated exactly from the more complicated equation (6), which does not necessarily imply conservation of entropy in the non-equilibrium case. The effect is found to be significant. Inclusion of the additional cooling of photons amplifies the neutrino spectral distortion by approximately 20% (see fig. 2). This can be explained as follows. The distortion of the spectrum is determined by the temperature difference $\Delta T/T_\nu = (T_\gamma - T_\nu)/T_\nu$ and by the strength of neutrino-electron interactions. The former rises with the expansion while the latter dies down. At large x the temperature difference ΔT is much larger than the correction to the photon temperature but at smaller $x = O(1)$ they do not differ so much. The dominant contribution to the distortion of the neutrino

spectrum comes just from the period when x is near unity and ΔT is relatively small, so that the small correction to T_γ is relatively enhanced. This effect was neglected in the previous papers [5, 7] so their results are somewhat underestimated; it was approximately calculated in ref. [6] under the assumption that the neutrinos have equilibrium spectra. However the spectral modification gives a contribution into additional photon cooling of the same order of magnitude and should be taken into account.

In the earlier papers [5, 6] the effect was considered in the Boltzmann approximation which simplifies the calculations very much. Another simplifying assumption, previously used, is the neglect of the electron mass in the collision integrals for νe -scattering and for annihilation $\bar{\nu}\nu \rightarrow e^+e^-$. We have also made numerical calculations in these approximations and found that both of these give rise to a larger spectral distortion in agreement with ref. [7]. In ref. [6] the effect was calculated numerically while in ref. [5] an approximate analytical expression was derived. However in ref. [5] the influence of the back-reactions which smoothes down the spectral distortion was underestimated due to a numerical error in the integral. With the correction of this error the effect should be twice smaller (in the approximations of that paper). Our numerical results in the limit of Boltzmann statistics and for $m_e = 0$ are in a reasonable agreement with the corrected estimate of that paper:

$$\delta_{\nu_e} \approx 3 \times 10^{-4} y(11y/4 - 3). \quad (15)$$

Acknowledgment. The work of AD and SH was supported in part by the Danish National Science Research Council through grant 11-9640-1 and in part by Danmarks Grundforskningsfond through its support of the Theoretical Astrophysical Center. The work of DS was supported in part by the Russian Foundation for Fundamental Research through grant 95-02-04911A and by the INTAS program of EC through grant INTAS-93-1630 (extension). DS thanks the Theoretical Astrophysical Center for hospitality during the last stages of this work.

A Reduction of the collision integral

In this Appendix we will make analytically as many integrations in the collision integral as possible. In the case we are interested in, *i.e.* four-particle interaction vertex and the isotropic one-particle distribution functions, seven out of nine integrations can be done and only two integrals upon the momentum remain for numerical treatment. We start from the general form of the collision integral in the space-homogeneous case:

$$I_{\text{coll}} = \frac{1}{2E_1} \int (2\pi)^4 \delta^4(\sum_i p_{\mu i}) |M_{fi}(|\mathbf{p}|)|^2 F(f) \prod_{i=2}^{i=4} \frac{d^3 \mathbf{p}_i}{(2\pi)^3 2E_i}, \quad (16)$$

where the particle energy is $E_i = \sqrt{m_i^2 + \mathbf{p}_i^2}$ and $F(f)$ is defined as:

$$F(f) = [1 - f_1][1 - f_2]f'_1 f'_2 - [1 - f'_1][1 - f'_2]f_1 f_2, \quad (17)$$

where the distribution functions f_j only depend upon the moduli of the particle momentum and time $f_j(|\mathbf{p}|, t)$. We make use of the identity:

$$\delta^3(\sum \mathbf{p}_i) = \int e^{i(\lambda, \mathbf{p}_1 + \mathbf{p}_2 - \mathbf{p}'_1 - \mathbf{p}'_2)} \frac{d^3 \lambda}{(2\pi)^3} \quad (18)$$

and explicitly separate out the angle integrations:

$$d^3 p_i = d\phi_i d\cos\theta_i p_i^2 dp_i \equiv p_i^2 dp_i d\Omega_i. \quad (19)$$

The collision integral in eq. (16) takes the form:

$$I_{\text{coll}} = \frac{1}{64\pi^3 E_1 p_1} \int \delta(E_1 + E_2 - E'_1 - E'_2) F(f) D(p_1, p_2, p'_1, p'_2) \frac{p'_1 dp'_1}{E'_1} \frac{p'_2 dp'_2}{E'_2} \frac{p_2 dp_2}{E_2}. \quad (20)$$

Here we have defined:

$$D(p_1, p_2, p'_1, p'_2) \equiv \frac{p_1 p_2 p'_1 p'_2}{64\pi^5} \int_0^\infty \lambda^2 d\lambda \int e^{i(\mathbf{p}_1, \lambda)} d\Omega_\lambda \int e^{i(\mathbf{p}_2, \lambda)} d\Omega_{p_2} \int e^{-i(\mathbf{p}'_1, \lambda)} d\Omega_{p'_1} \int e^{-i(\mathbf{p}'_2, \lambda)} d\Omega_{p'_2} |M_{fi}(|\mathbf{p}|)|^2. \quad (21)$$

In the four-fermion approximation all the possible squared matrix elements consist of two kinds of terms:

$$K_1(q_{1,\mu} q_2^\mu)(q_{3,\nu} q_4^\nu) = K_1(E_1 E_2 - \vec{q}_1 \vec{q}_2)(E_3 E_4 - \vec{q}_3 \vec{q}_4) \quad (22)$$

and:

$$K_2 m^2(q_{3\mu} q_4^\mu) = K_2 m^2(E_3 E_4 - \vec{q}_3 \vec{q}_4) , \quad (23)$$

where every q_i corresponds to some of p_i . In order to perform the angle integrals we define the angles between \vec{q}_i through angles from eq. (21) as:

$$\cos \phi_{12} = \sin \theta_1 \sin \theta_2 \cos(\varphi_1 - \varphi_2) + \cos \theta_1 \cos \theta_2 . \quad (24)$$

The integration in the angles φ_1 or φ_2 over the total period and the structure of the matrix elements in eqs. (22,23) result in the vanishing of the first term in eq. (24). Then all angle integrals in eq. (21) can be trivially taken and we come to three kinds of integrals⁶:

$$D_1 = \frac{4}{\pi} \int_0^\infty \frac{d\lambda}{\lambda^2} \sin(\lambda q_1) \sin(\lambda q_2) \sin(\lambda q_3) \sin(\lambda q_4) , \quad (25)$$

$$D_2(3, 4) = \frac{4q_3 q_4}{\pi} \int_0^\infty \frac{d\lambda}{\lambda^2} \sin(\lambda q_1) \sin(\lambda q_2) \left[\cos(\lambda q_3) - \frac{\sin(\lambda q_3)}{\lambda q_3} \right] \left[\cos(\lambda q_4) - \frac{\sin(\lambda q_4)}{\lambda q_4} \right] , \quad (26)$$

and:

$$D_3 = \frac{4q_1 q_2 q_3 q_4}{\pi} \int_0^\infty \frac{d\lambda}{\lambda^2} \left[\cos(\lambda q_1) - \frac{\sin(\lambda q_1)}{\lambda q_1} \right] \left[\cos(\lambda q_2) - \frac{\sin(\lambda q_2)}{\lambda q_2} \right] \left[\cos(\lambda q_3) - \frac{\sin(\lambda q_3)}{\lambda q_3} \right] \left[\cos(\lambda q_4) - \frac{\sin(\lambda q_4)}{\lambda q_4} \right] \quad (27)$$

For the matrix element squared given by eq. (22) the function D in eq. (21) can be written in the form:

$$D = K_1 (E_1 E_2 E_3 E_4 D_1 + D_3) + K_1 [E_1 E_2 D_2(3, 4) + E_3 E_4 D_2(1, 2)] , \quad (28)$$

while for the matrix element squared given by eq. (23) we get:

$$D = K_2 E_1 E_2 [E_3 E_4 D_1 + D_2(3, 4)] . \quad (29)$$

⁶In the case that one of q_3 or q_4 in the second integral D_2 corresponds to the incoming particle and the other to the outgoing one, D_2 changes sign.

The calculation of the integrals (25-27) is straightforward. The functions D_1 and D_3 are symmetric with respect to permutations of any variables and D_2 is symmetric under permutations $1 \leftrightarrow 2$ and $3 \leftrightarrow 4$. In what follows we present the expression for $D_2(3, 4)$. Without loss of generality we can assume that $q_1 > q_2$ and $q_3 > q_4$. Then we will have four different cases, which depend upon relations between the momenta.⁷

a) $q_1 + q_2 > q_3 + q_4$ and $q_1 + q_4 > q_2 + q_3$,

$$D_1 = \frac{1}{2}(q_2 + q_3 + q_4 - q_1) \quad (30)$$

$$D_2 = \frac{1}{12}((q_1 - q_2)^3 + 2(q_3^3 + q_4^3) - 3(q_1 - q_2)(q_3^2 + q_4^2)) , \quad (31)$$

$$\begin{aligned} D_3 = & \frac{1}{60} \left(q_1^5 - 5q_1^3q_2^2 + 5q_1^2q_2^3 - q_2^5 \right. \\ & - 5q_1^3q_3^2 + 5q_2^3q_3^2 + 5q_1^2q_3^3 + 5q_2^2q_3^3 - q_3^5 - 5q_1^3q_4^2 \\ & \left. + 5q_2^3q_4^2 + 5q_3^3q_4^2 + 5q_1^2q_4^3 + 5q_2^2q_4^3 + 5q_3^2q_4^3 - q_4^5 \right) \end{aligned} \quad (32)$$

b) $q_1 + q_2 > q_3 + q_4$ and $q_1 + q_4 < q_2 + q_3$,

$$D_1 = q_4 \quad (33)$$

$$D_2 = \frac{1}{3}q_4^3 , \quad (34)$$

$$D_3 = \frac{1}{30}q_4^3 (5q_1^2 + 5q_2^2 + 5q_3^2 - q_4^2) \quad (35)$$

c) $q_1 + q_2 < q_3 + q_4$ and $q_1 + q_4 < q_2 + q_3$,

$$D_1 = \frac{1}{2}(q_1 + q_2 + q_4 - q_3) \quad (36)$$

⁷In the general case there are two other possibilities $q_1 > q_2 + q_3 + q_4$ and $q_3 > q_1 + q_2 + q_4$. However they are unphysical and give zero answer for all integrals, $D_1 = D_2 = D_3 = 0$.

$$D_2 = \frac{1}{12} (-(q_1 + q_2)^3 - 2q_3^3 + 2q_4^3 + 3(q_1 + q_2)(q_3^2 + q_4^2)) , \quad (37)$$

D_3 is the same as eq. (32) but with the change of variables $1 \leftrightarrow 3$ and $2 \leftrightarrow 4$.

d) $q_1 + q_2 < q_3 + q_4$ and $q_1 + q_4 > q_2 + q_3$,

$$D_1 = q_2 \quad (38)$$

$$D_2 = \frac{1}{6} q_2 (3q_3^2 + 3q_4^2 - 3q_1^2 - q_2^2) , \quad (39)$$

$$D_3 = \frac{1}{30} q_2^3 (5q_1^2 + 5q_3^2 + 5q_4^2 - q_2^2) \quad (40)$$

Now, the energy δ -function can be trivially integrated away and we are left with the following two-dimensional integral upon energies of incoming particles:

$$\frac{df(E_1, t)}{dt} = \frac{1}{64\pi^3 E_1 p_1} \int \int F(f) (\sum_k D_k) \frac{p'_1 dp'_1}{E'_1} \frac{p'_2 dp'_2}{E'_2} , \quad (41)$$

where $E_2 = E'_1 + E'_2 - E_1$, $p_2 = \sqrt{E_2^2 - m_2^2}$ and the summation in eq. (41) is made over all D_k contributing to the squared matrix elements in eqs. (22,23). In the integration one should take into account the θ -functions corresponding to the cases a)-d) as well as the θ -function related to the energy conservation, $\theta(E_3 + E_4 - E_1 - m_2)$.

We can further check our calculations of the D functions, using the following trick. In the case $m_1^2 + m_2^2 = m_3^2 + m_4^2$ the l.h.s. of the eq. (22) can be rewritten as:

$$K_1(q_{1\mu} q_2^\mu)(q_{3\nu} q_4^\nu) = K_1(q_{3\mu} q_4^\mu)^2 . \quad (42)$$

We can now integrate the r.h.s. of eq. (42) over angles. Consequently we obtain integrals in the form of eqs. (25,26) and one more integral:

$$D_4(3, 4) = \frac{4q_3^2 q_4^2}{\pi} \int_0^\infty \frac{d\lambda}{\lambda^2} \sin(\lambda q_1) \sin(\lambda q_2) \left[\sin(\lambda q_3) - \frac{2}{\lambda q_3} \left(\cos(\lambda q_3) - \frac{\sin(\lambda q_3)}{\lambda q_3} \right) \right] \\ \left[\sin(\lambda q_4) - \frac{2}{\lambda q_4} \left(\cos(\lambda q_4) - \frac{\sin(\lambda q_4)}{\lambda q_4} \right) \right] \quad (43)$$

The equivalence of the two approaches requires that the following two conditions should be fulfilled:

$$D_2(1, 2) \equiv \frac{p_1^2 + p_2^2 - p_3^2 - p_4^2}{2} D_1 + D_2(3, 4) , \quad (44)$$

and

$$D_3 \equiv \frac{p_1^2 + p_2^2 - p_3^2 - p_4^2}{2} D_2(3, 4) + D_4(3, 4) . \quad (45)$$

We have checked that this is indeed true, and thus assured that the D functions have been calculated correctly.

B The collision integrals in the Boltzmann approximation

We have also checked the correctness of our calculations in the following way. In the Boltzmann approximation we have calculated everything twice, first letting the computer solve the equations directly, and second, by using different exact expressions in a half of the collision integral. In the Boltzmann approximation we reduced the first half of the collision integrals to the following one dimensional integrals over momentum.

For the reactions $\nu_e \nu_e \rightarrow \nu_e \nu_e$ and $\nu_e \bar{\nu}_e \rightarrow \nu_e \bar{\nu}_e$ the first half of the collision integral is:

$$\begin{aligned} I_{Coll} &= \frac{2^5 G_F^2}{2E_1} \int \frac{d^3 q_2 d^3 q_3 d^3 q_4}{(2\pi)^9 8 E_2 E_3 E_4} (2\pi)^4 \delta^4(q_1 + q_2 - q_3 - q_4) \cdot F(f) \cdot \\ &\quad \cdot [2(q_1 \cdot q_2)^2 + 4(q_1 \cdot q_4)^2] \\ &= \frac{20 G_F^2}{9\pi^3} E_1 \int dE_2 E_2^2 \cdot F(f), \end{aligned}$$

where $F(f) = [-f_{(in\ 1)} f_{(in\ 2)}]$ with f_{in} being the distribution functions for the incoming particles.

For the first 5 reactions in Table 1 (including neutrinos only) we obtain the result:

$$I_{coll}^{first\ 5} = \frac{8G_F^2}{3\pi^3} \int dp_2 p_2^3 \left[-f_{\nu_e}(1) \left(f_{\nu_e}(2) + \frac{2}{3} f_{\nu_\mu}(2) \right) \right]. \quad (46)$$

The reaction $\nu_e \bar{\nu}_e \rightarrow e^+ e^-$ gives:

$$I_{Coll}^{\nu_e \bar{\nu}_e} = \frac{G_F^2}{\pi^3} E_1 \int d\xi dp_2 p_2^3 \sqrt{1 - \frac{4m_e^2}{s} (1 - \xi)^2} \cdot [-f_{\nu_e}(1) f_{\nu_e}(2)] \cdot \left[\frac{1}{3} (g_L^2 + g_R^2) \left(1 - \frac{m_e^2}{s} \right) + 2g_L g_R \frac{m_e^2}{s} \right], \quad (47)$$

where $s = 2E_1 E_2 (1 - \xi)$ is expressed through the angle $\xi = \cos \theta_{12}$ between the incoming particles.

The reactions $\nu_e e^\pm \rightarrow \nu_e e^\pm$ give:

$$I_{coll}^{\nu_e e^\pm} = \frac{G_F^2}{\pi^3} \int d\xi dp_2 p_2^2 \frac{1 - \frac{m_e^2}{s}}{E_1 E_2} (p_1 \cdot p_2)^2 [-f_{\nu_e}(1) f_e(2)] \cdot \left[\frac{1}{3} (g_L^2 + g_R^2) \left(4 + \frac{m_e^2}{s} \left(1 + \frac{m_e^2}{s} \right) \right) - 2g_L g_R \frac{m_e^2}{s} \right] \quad (48)$$

where $s = 2E_1 E_2 (1 - \beta \xi) + m_e^2$ and β is the velocity of the incoming electron (positron). As always we have defined $g_L = 1/2 + \sin^2 \theta_W$ and $g_R = \sin^2 \theta_W$. The angle integrals are easily done, giving for the $\nu_e e^\pm$ case:

$$I_{coll}^{\nu_e e^\pm} = \frac{G_F^2}{16\pi^2} \int_0^\infty dp_2 \frac{p_2}{E_1 E_2} [-f_{\nu_e}(1) f_e(2)] m_e^6 \cdot \left[2(g_L^2 + g_R^2) \left(\frac{1}{6u^2} + \frac{1}{u} + \frac{10u}{3} - \frac{11u^2}{6} + \frac{4u^3}{9} - \frac{4}{3} \log(u) \right) + 4g_L g_R \left(\frac{2}{3u} - 3u + \frac{u^2}{2} + 3 \log(u) \right) \right], \quad (49)$$

where $u = s/m_e^2$.

Similarly for the interactions of muonic neutrinos with themselves or other neutrinos, which are the first 5 reactions in Table 2, we get:

$$I_{coll}^{first\ 5\ \nu_\mu} = \frac{8G_F^2}{9\pi^2} E_1 \int dp_2 p_2^3 \left[-f_{\nu_\mu}(1) \left(4f_{\nu_\mu}(2) + f_{\nu_e}(2) \right) \right]. \quad (50)$$

For the interactions of ν_μ with electrons we obtain the same expression as for ν_e except for the change $g_L \rightarrow \tilde{g}_L = g_L - 1$ and the substitution like $f_{\nu_e} \rightarrow f_{\nu_\mu}$.

Process		$2^{-5}G_F^{-2}S A ^2$
$\nu_e + \bar{\nu}_e$	$\rightarrow \nu_e + \bar{\nu}_e$	$4(p_1 \cdot p_4)(p_2 \cdot p_3)$
$\nu_e + \nu_e$	$\rightarrow \nu_e + \nu_e$	$2(p_1 \cdot p_2)(p_3 \cdot p_4)$
$\nu_e + \bar{\nu}_e$	$\rightarrow \nu_{\mu(\tau)} + \bar{\nu}_{\mu(\tau)}$	$(p_1 \cdot p_4)(p_2 \cdot p_3)$
$\nu_e + \bar{\nu}_{\mu(\tau)}$	$\rightarrow \nu_e + \bar{\nu}_{\mu(\tau)}$	$(p_1 \cdot p_4)(p_2 \cdot p_3)$
$\nu_e + \nu_{\mu(\tau)}$	$\rightarrow \nu_e + \nu_{\mu(\tau)}$	$(p_1 \cdot p_2)(p_3 \cdot p_4)$
$\nu_e + \bar{\nu}_e$	$\rightarrow e^+ + e^-$	$4[(g_L^2(p_1 \cdot p_4)(p_2 \cdot p_3)$ $+ g_R^2(p_1 \cdot p_3)(p_2 \cdot p_4)$ $+ g_L g_R m_e^2(p_1 \cdot p_2)]$
$\nu_e + e^-$	$\rightarrow \nu_e + e^-$	$4[g_L^2(p_1 \cdot p_2)(p_3 \cdot p_4)$ $+ g_R^2(p_1 \cdot p_4)(p_2 \cdot p_3)$ $- g_L g_R m_e^2(p_1 \cdot p_3)]$
$\nu_e + e^+$	$\rightarrow \nu_e + e^+$	$4[g_R^2(p_1 \cdot p_2)(p_3 \cdot p_4)$ $+ g_L^2(p_1 \cdot p_4)(p_2 \cdot p_3)$ $- g_L g_R m_e^2(p_1 \cdot p_3)]$

Table 1: The matrix elements for various processes with electronic neutrinos; here $g_L = 1/2 + \sin^2 \theta_W$ and $g_R = \sin^2 \theta_W$.

Process		$2^{-5}G_F^{-2}S A ^2$
$\nu_\mu + \bar{\nu}_\mu$	$\rightarrow \nu_\mu + \bar{\nu}_\mu$	$4(p_1 \cdot p_4)(p_2 \cdot p_3)$
$\nu_\mu + \nu_\mu$	$\rightarrow \nu_\mu + \nu_\mu$	$2(p_1 \cdot p_2)(p_3 \cdot p_4)$
$\nu_\mu + \bar{\nu}_\mu$	$\rightarrow \nu_{e(\tau)} + \bar{\nu}_{e(\tau)}$	$(p_1 \cdot p_4)(p_2 \cdot p_3)$
$\nu_\mu + \bar{\nu}_{e(\tau)}$	$\rightarrow \nu_\mu + \bar{\nu}_{e(\tau)}$	$(p_1 \cdot p_4)(p_2 \cdot p_3)$
$\nu_\mu + \nu_{e(\tau)}$	$\rightarrow \nu_\mu + \nu_{e(\tau)}$	$(p_1 \cdot p_2)(p_3 \cdot p_4)$
$\nu_\mu + \bar{\nu}_\mu$	$\rightarrow e^+ + e^-$	$4[(\tilde{g}_L^2(p_1 \cdot p_4)(p_2 \cdot p_3)$ $+ g_R^2(p_1 \cdot p_3)(p_2 \cdot p_4)$ $+ \tilde{g}_L g_R m_e^2(p_1 \cdot p_2)]$
$\nu_\mu + e^-$	$\rightarrow \nu_\mu + e^-$	$4[\tilde{g}_L^2(p_1 \cdot p_2)(p_3 \cdot p_4)$ $+ g_R^2(p_1 \cdot p_4)(p_2 \cdot p_3)$ $- \tilde{g}_L g_R m_e^2(p_1 \cdot p_3)]$
$\nu_\mu + e^+$	$\rightarrow \nu_\mu + e^+$	$4[g_R^2(p_1 \cdot p_2)(p_3 \cdot p_4)$ $+ \tilde{g}_L^2(p_1 \cdot p_4)(p_2 \cdot p_3)$ $- \tilde{g}_L g_R m_e^2(p_1 \cdot p_3)]$

Table 2: The matrix elements for various processes with muonic or tau neutrinos; here $\tilde{g}_L = g_L - 1 = -1/2 + \sin^2 \theta_W$ and $g_R = \sin^2 \theta_W$.

Program	T_γ/T_ν	$\delta\rho_{\nu e}/\rho_{\nu e}$	$\delta\rho_{\nu\mu(\tau)}/\rho_{\nu\mu(\tau)}$
Full distribution f(x,y) momentum points 100 initial time $x_{in} = 0.2$ Bulirsch-Stoer method [9]	1.3996	0.80 %	0.26 %
Full distribution f(x,y) momentum points 100 initial time $x_{in} = 0.1$ Simple time evolution	1.3996	0.79 %	0.25 %
Full distribution f(x,y) momentum points 200 initial time $x_{in} = 0.1$ Simple time evolution	1.3994	0.83 %	0.33 %
Correction $\delta(x, y)$ momentum points 200 initial time $x_{in} = 0.1$ Simple time evolution	1.3991	0.94 %	0.40 %
Same, but assuming entropy conservation (photon cooling due to νe -interaction is neglected)	1.4010	1.13 %	0.53 %

Table 3: Comparison of the results of different ways of calculation. All the results are for FD case.

References

- [1] S. Weinberg, *Gravitation and Cosmology*, Wiley, New York, 1972.
- [2] D.A. Dicus, E.W. Kolb, A.M. Gleeson, E.C.G. Sudarshan, V.L. Teplits, and M.S. Turner, *Phys. Rev. D* **26** (1982) 2694.
- [3] M.A. Herrera and S. Hacyan, *Astrophys. J.* **336** (1989) 539; *Phys. Fluids*, **28** (1985) 3253.
- [4] N.C. Raha and B. Mitra, *Phys. Rev. D* **44** (1991) 393.
- [5] A.D. Dolgov and M. Fukugita, *JETP Lett.* **56** (1992) 123; *Phys. Rev. D* **46** (1992) 5378.
- [6] S. Dodelson and M.S. Turner, *Phys. Rev. D* **46** (1992) 3372.
- [7] S. Hannestad and J. Madsen, *Phys. Rev. D* **52** (1995) 1764.
- [8] D.V. Semikoz and I.I. Tkachev, *Phys. Rev. Lett.* **74**, 3093 (1995); D.V. Semikoz and I.I. Tkachev, hep-ph/9507306, to appear in *Phys.Rev.D*.
- [9] W.H.Press et al., “*Numerical Recipes in C: the art of scientific computing*”, Cambridge U. Press, 1992.
- [10] L. Kawano, Fermilab-Pub-92/04-A (1992).

Figure Captions:

Fig. 1 The ratio T_γ/T_ν as a function of the dimensionless "time" $x = ma$ for the cases of Fermi-Dirac and Maxwell-Boltzmann statistics. The value $x = 1$ corresponds to $T_\nu = 1MeV$.

Fig. 2 The relative distortion of the total neutrino energy density $\delta\rho/\rho_{eq}$ (for the definition see eq. (11)) as a function of $x = ma$ for the case of "entropy conservation" (upper curve) and energy conservation according to eq. (6) (lower curve). In the first case we neglect the energy exchange between neutrinos and e^\pm which is equivalent to the requirement of entropy conservation in the electromagnetic plasma.

Fig. 3 The "time" evolution of the correction to the neutrino distribution functions $\delta_j = (f_{\nu_j} - f_\nu^{eq})/f_\nu^{eq}$ for several fixed values of momentum $y = 3, 5, 7$. In Fig.3a and 3b we present respectively the results for electronic neutrinos, and for muonic (tau) ones.

Fig. 4 The evolution of the non-equilibrium corrections to the distribution functions for the momentum value $y = 5$ for the electronic (solid curve) and muonic (tau) (dotted curve) neutrinos in the cases of FD and MB statistics.

Fig. 5 The distortion of the neutrino spectra $\delta_j = (f_{\nu_j} - f_\nu^{eq})/f_\nu^{eq}$ as functions of the dimensionless momentum y at the final "time" $x = 60$. The dashed lines a and c correspond to Maxwell-Boltzmann statistics, while the solid lines b and d correspond to Fermi-Dirac statistics. The upper curves a and b are for electronic neutrinos, while the lower curves c and d are for muonic (tau) neutrinos. All the curves can be well approximated by a second order polynomial in y like $\delta = Ay(y - B)$.

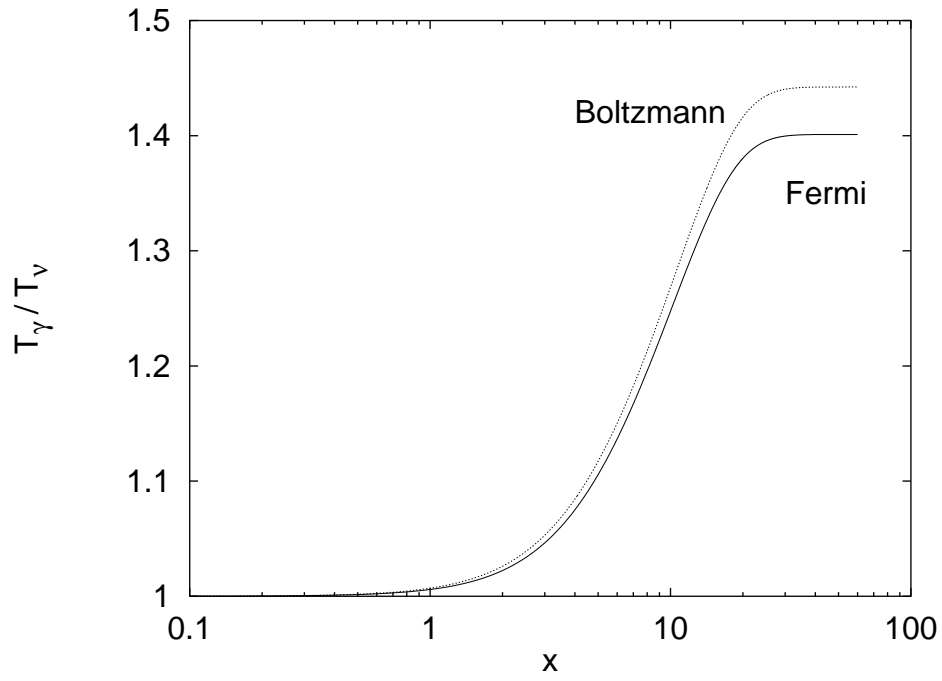


Figure 1.

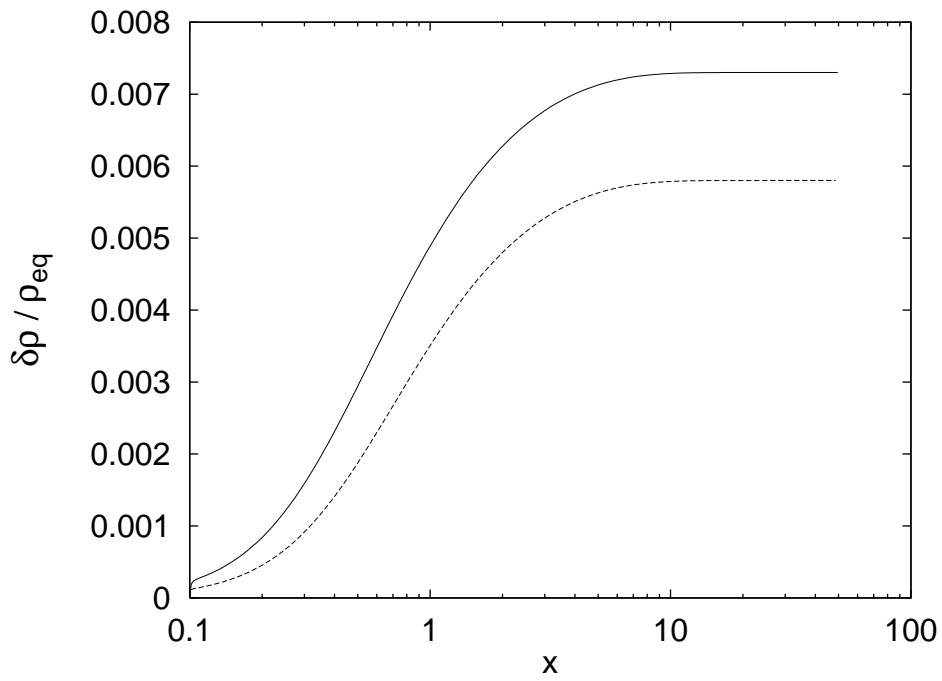


Figure 2.

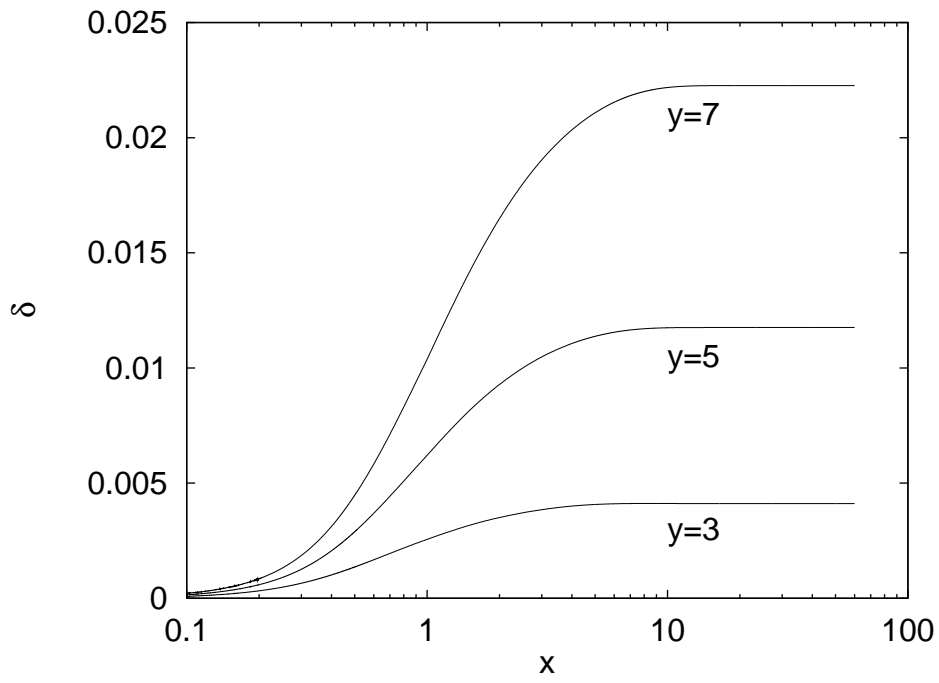


Figure 3a.

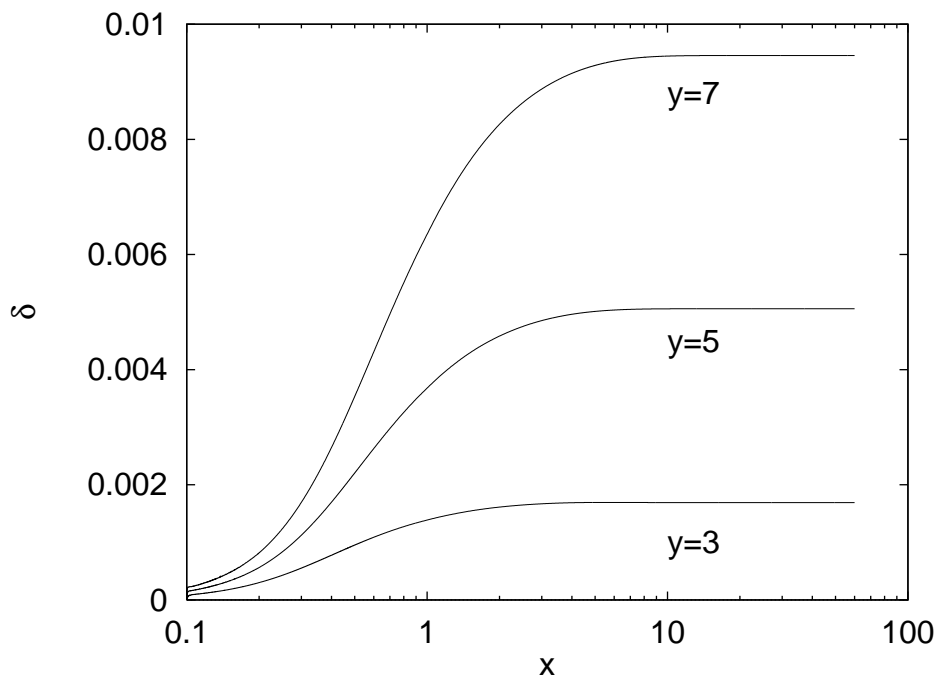


Figure 3b.

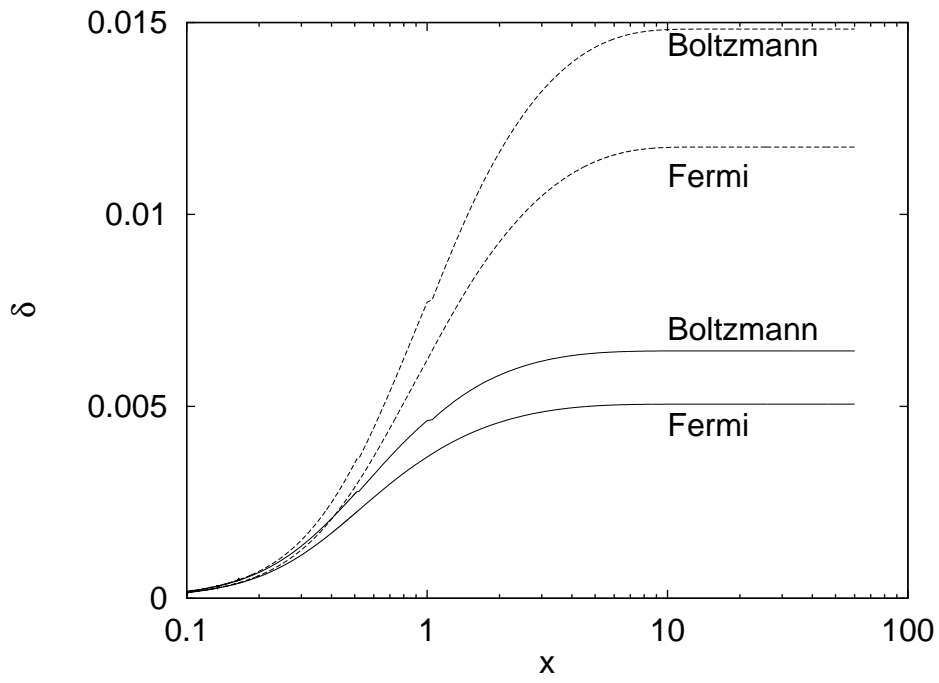


Figure 4.

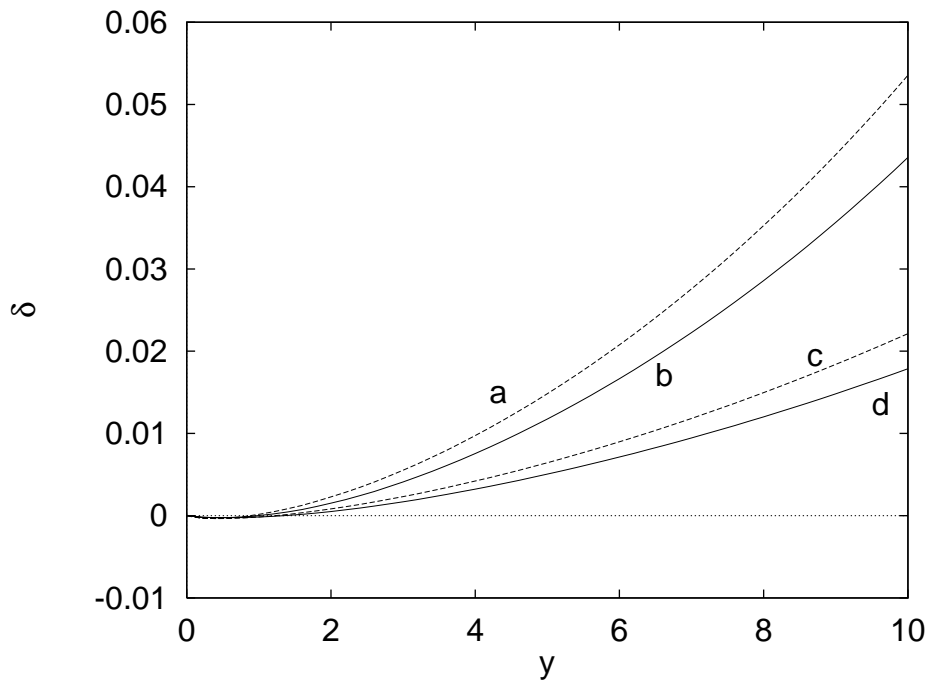


Figure 5.